Journal of Biomechanics 46 (2013) 1031–1034

Contents lists available at SciVerse ScienceDirect

Journal of Biomechanics

journal homepage: www.elsevier.com/locate/jbiomech
www.JBiomech.com

Short communication

A thumb carpometacarpal joint coordinate system based on articular surface geometry

Eni Halilaj [a], Michael J. Rainbow [b], Christopher J. Got [c], Douglas C. Moore [c], Joseph J. Crisco [a,c,*]

[a] Center for Biomedical Engineering and School of Engineering, Brown University, Providence, RI 02912, USA
[b] Department of Physical Medicine and Rehabilitation, Harvard Medical School, Cambridge, MA 02138, USA
[c] Department of Orthopaedics, The Warren Alpert Medical School of Brown University and Rhode Island Hospital, Providence, RI 02903, USA

ARTICLE INFO

Article history:
Accepted 6 December 2012

Keywords:
Articular geometry
Thumb CMC
Anatomical coordinate system
Kinematics
Computed tomography
3-dimensional models

ABSTRACT

The thumb carpometacarpal (CMC) joint is a saddle-shaped articulation whose *in vivo* kinematics can be explored more accurately with computed tomography (CT) imaging methods than with previously used skin-based marker systems. These CT-based methods permit a detailed analysis of the morphology of the joint, and thus the prominent saddle geometry can be used to define a coordinate system that is inherently aligned with the primary directions of motion at the joint. The purpose of this study was to develop a CMC joint coordinate systems that is based on the computed principal directions of curvature on the trapezium and the first metacarpal. We evaluated the new coordinate system using bone surface models segmented from the CT scans of 24 healthy subjects. An analysis of sensitivity to the manual selection of articular surfaces resulted in mean orientation differences of $0.7 \pm 0.7^{\circ}$ and mean location differences of 0.2 ± 0.1 mm. Inter-subject variability, which mostly emanates from anatomical differences, was evaluated with whole bone registration and resulted in mean orientation differences of $3.1 \pm 2.7^{\circ}$ and mean location differences of 0.9 ± 0.5 mm. The proposed joint coordinate system addresses concerns of repeatability associated with bony landmark identification and provides a robust platform for describing the complex kinematics of the CMC joint.

1. Introduction

Motion of the thumb is greatly influenced by the articular geometry of the thumb carpometacarpal (CMC) joint—a well-defined saddle that facilitates flexion/extension and adduction/abduction, while partly restraining axial rotation (Chèze et al., 2012; Cooney et al., 1981; Hollister et al., 1992; Imaeda et al., 1994; Pieron, 1973). The range of motion at the CMC joint has been reported to be approximately 53° of flexion/extension, 42° of adduction/abduction, and 17° of axial rotation (Cooney et al., 1981), reflecting the fact that flexion/extension and adduction/abduction are the primary physiological motions in this joint. Other studies have also determined that the primary axes of rotation at the CMC joint are closely aligned with its saddle geometry (Hollister et al., 1992; Imaeda et al., 1994).

The International Society of Biomechanics (ISB) has proposed standardized joint coordinate systems (JCS) for various joints in the human body (Wu et al., 2005), based on Grood and Suntay's knee coordinate system (Grood and Suntay, 1983) which consists of two body-fixed axes—one axis embedded in each bone—and a floating axis that is perpendicular to each of the body-fixed axes. In order to minimize cross-talk in kinematic data reporting, the rotational axis with the least physiological motion should be defined as the floating axis of the JCS. In the knee, adduction/abduction is considerably minor when compared to the other two rotations, and therefore is defined as the floating axis (Grood and Suntay, 1983). However, applying an analogous coordinate system to the thumb CMC joint is not optimal because internal/external rotation of the metacarpal is the smallest physiological rotation. Hence, Cheze et al. (2009) proposed a refinement of the ISB-recommended CMC JCS, in which the flexion/extension and the adduction/abduction axes are the body-fixed axes and the internal/external rotation axis is floating. Using an experimental model, they also demonstrated that their recommended sequence reduced cross-talk among the three rotational motions.

Given an optimal Euler sequence (Cheze et al., 2009), the next step towards a more robust CMC JCS is a rigorous definition of the body-fixed flexion/extension and adduction/abduction axes. Since motion at the CMC joint is governed by the saddle geometry of its articular surfaces, previous CMC joint coordinate systems

* Correspondence to: Bioengineering Laboratory, Department of Orthopaedics, The Warren Alpert Medical School of Brown University and Rhode Island Hospital, 1 Hoppin Street, CORO West, Suite 404, Providence, RI 02903, USA.
Tel.: +1 401 444 4231; fax: +1 401 444 4418.
E-mail address: joseph_crisco@brown.edu (J.J. Crisco).

0021-9290/$ - see front matter © 2013 Elsevier Ltd. All rights reserved.
http://dx.doi.org/10.1016/j.jbiomech.2012.12.002

(Cheze et al., 2009; Cooney et al., 1981; Wu et al., 2005) have been based on anatomical landmarks that seek to align the flexion/extension axis with the concavity and the adduction/abduction axis with the convexity of the saddle-shaped joint. Although axes derived from anatomical landmarks may approximate the concavity and the convexity of the articular surfaces at the CMC joint, the subjective process of landmark selection has limitations. The kinematic errors associated with landmark imprecision have created a need for coordinate system definitions that are intrinsically robust (Della Croce et al., 2005). In the CMC joint, computation of the principal directions of curvature directly from the articular topography rather than through approximation, presents an opportunity for improved accuracy and repeatability.

In this communication we present a semi-automated method for generating a thumb CMC joint coordinate system that is based on the computed principal directions of curvature in the articulation and therefore avoids potential limitations associated with manual landmark identification. We supplement our proposed method with sensitivity and inter-subject variability analyses of *in vivo* data from a set of 24 healthy joints.

2. Methods

2.1. 3D bone models

After receiving approval from the Institutional Review Board and obtaining informed consents, the wrists and thumbs on the dominant hands of 24 healthy volunteers (12 males, age 38.7 ± 11.7 yrs and 12 females, age 43.2 ± 15.8 yrs) were imaged in a clinical neutral position with a 16-slice clinical CT scanner (GE LightSpeed 16, General Electric, Milwaukee, WI). Imaging parameters included tube settings of 80 kVp and 80 mA, slice thickness of 0.625 mm, and in-plane resolution of at least 0.4 mm × 0.4 mm. The trapeziae and the first metacarpals were segmented using Mimics v12.11 (Materialise, Leuven, Belgium) and 3-D bone models were exported as meshed surfaces.

2.2. Segment coordinate system (SCS) generation

The trapezial and the metacarpal segment coordinate systems were based on the principal directions of curvature on the articular surfaces of each 3-D bone model. The borders of the articular surfaces were manually selected in Geomagic Studio (Geomagic, Research Triangle Park, NC) by carefully tracing the visible perimeter of the subchondral bone surfaces (Fig. 1a). A monotone fifth order polynomial surface ($f(x,y)$) was fit to each selected articular surface. The local saddle point ($f(a,b)$) was determined by computing the gradient fields (Fig. 1b), finding the critical points, and performing a second partial derivative test:

$$if \begin{vmatrix} f_{xx}(a,b) & f_{xy}(a,b) \\ f_{yx}(a,b) & f_{yy}(a,b) \end{vmatrix} < 0, \text{then } f(a,b) \text{ is a saddle point.}$$

A fifth order polynomial surface was chosen because it was the lowest order polynomial with a root-mean-squared (RMS) error of less than 0.1 mm, capturing the salient global features of the saddle while avoiding over-fitting, which includes local features that are of little importance to overall joint motion. Principal directions of curvature were computed for the portion of the surface within 3 mm of the saddle point, and their vector averages—$\boldsymbol{i}$ in the direction of minimum curvature and $\boldsymbol{k}$ in the direction of maximum curvature – were computed (Fig. 1c). The 3 mm threshold was chosen because the bounded points captured the saddle geometry and excluded regions of high shape variation at the edges of the articular surfaces.

Following the ISB convention (Wu and Cavanagh, 1995; Wu et al., 2005), the *z*-axis of the trapezial coordinate system (Z_{TPM}) was defined by $\boldsymbol{i}_{TPM}$, running in a ulnar-to-radial direction, the *y*-axis (Y_{TPM}) by the cross product of Z_{TPM} and $\boldsymbol{k}_{TPM}$, oriented in a distal-to-proximal direction, and the *x*-axis (X_{TPM}) by the cross product of Y_{TPM} and Z_{TPM}, running in a dorsal-to-volar direction. Similarly, X_{MC1} in the metacarpal coordinate system was defined by $\boldsymbol{i}_{MC1}$, Y_{MC1} by the cross product of $\boldsymbol{k}_{MC1}$ and X_{MC1}, and Z_{MC1} as the cross product of the X_{MC1} and the Y_{MC1} (Fig. 1c). The saddle point, served as the origin of each segment coordinate system.

2.3. Joint coordinate system (JCS) definition

Based on the axes of rotation of an idealized saddle (Fig. 2), joint flexion/extension is defined as rotation about the trapezial-fixed Z_{TPM} and joint abduction/adduction as rotation about the metacarpal-fixed X_{MC1}; internal/external rotation then corresponds to rotation about the floating axis (Fig. 3). Using the *ZYX* Euler sequence, this configuration minimizes angular cross-talk in the CMC joint (Cheze et al., 2009). Consistent with the ISB guidelines (Wu et al., 2005), the neutral posture is defined as the position where the axes of the two segment coordinate systems are aligned, and translation of the metacarpal with respect to the trapezium is defined as the translation of the MC1 SCS origin with respect to the TPM SCS.

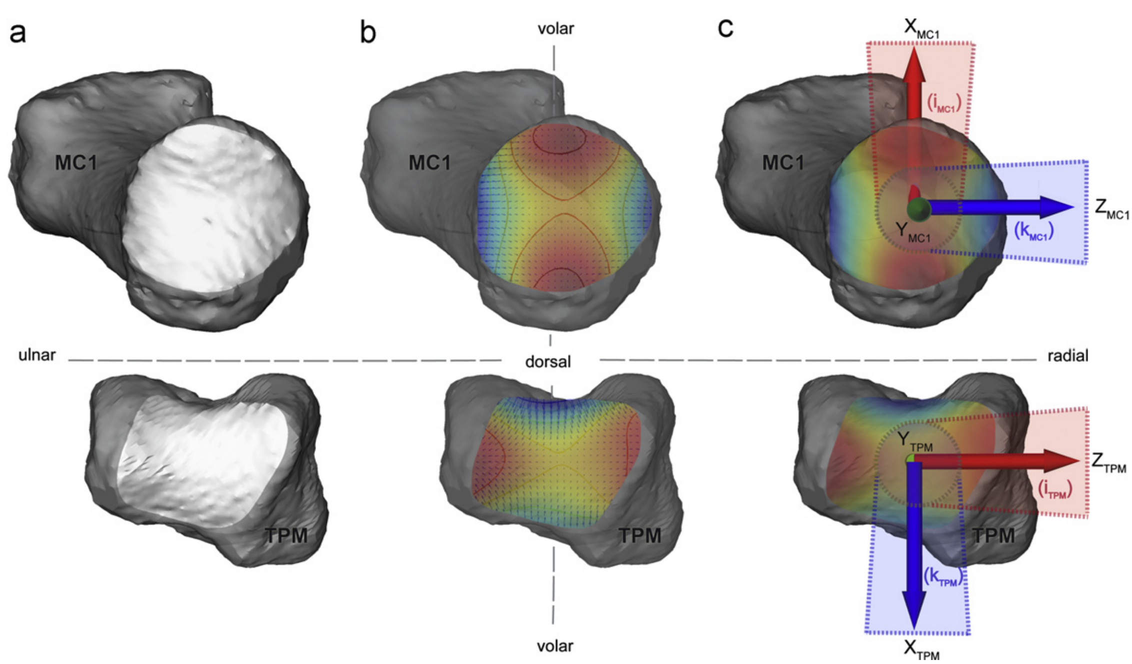

Fig. 1. Exploded views of the trapezium (TPM) and the first metacarpal (MC1) with: (a) the manually-selected subchondral bone surfaces, (b) the 5th order polynomial fits to the articular surfaces, colored by elevation, isocontours of the articular topography, and gradient fields (∇f; at the saddle point, $\nabla f=0$ and the determinant of the Hessian is less than 0), (c) the trapezial and the metacarpal coordinate systems, where $\boldsymbol{i}$ and $\boldsymbol{k}$ are the average principal direction vectors for points within a 3 mm radius from the saddle point, $Z_{TPM}= \boldsymbol{i}_{TPM}$; $Y_{TPM}= Z_{TPM} \times \boldsymbol{k}_{TPM}$; $X_{TPM}=Y_{TPM} \times Z_{TPM}$; $X_{MC1}= \boldsymbol{i}_{MC1}$; $Y_{MC1}=\boldsymbol{k}_{MC1} \times X_{MC1}$; $Z_{MC1}=X_{MC1} \times Y_{MC1}$.